Korean J. Chem. Eng., **25**(4), 780-786 (2008)

NH_3 removal using the dielectric barrier discharge plasma-V-TiO_2 photocatalytic hybrid system

Ji-Young Ban*, Hyun Il Kim*, Suk-Jin Choung*, Harim Jeong, and Misook Kang**,†**

*Department of Chemical Engineering, School of Environmental Applied Chemistry, KyungHee University, Yongin, Gyeonggi 449-701, Korea
**Department of Chemistry, College of Science, Yeungnam University, Gyeongsan, Gyeongbuk 712-749, Korea
(*Received 12 September 2007 • accepted 29 February 2008*)

Abstract−This study investigates the photocatalytic performance of V-TiO_2 for removal of highly concentrated ammonia (1,000 ppm) in the dielectric barrier discharge (DBD), plasma-photocatalytic, hybrid system. The V (1.0, 5.0, 10.0 mol-%)-TiO_2 photocatalysts were prepared by using the conventional sol-gel method. Their surface areas were decreased with increasing vanadium component. The UV-visible absorption band slightly shifted to more visible wavelengths in V-TiO_2 compared to that in pure TiO_2. The NH_3-TPD result confirmed that the ability of NH_3 adsorption on the surface of V-TiO_2 increased with increasing vanadium content, and was maximized for 5.0-mol% V-TiO_2. The NH_3 decomposition was enhanced with the photocatalyst compared to the decomposition rate without catalysts, while the decomposition was further increased with the applied plasma voltage. The NH_3 decomposition reached 90% after 400 min at an applied plasma voltage of 10.0 kV, and various intermediates, such as -NH_2, -NH, and NO, were also identified by using the Fourier transform infrared (FT-IR) spectra. In addition, the NH_3 decomposition reached 100% in the plasma-5.0 mol% V-TiO_2, photocatalytic, hybrid system after 25 min, compared to 98% in the pure V-TiO_2 photocatalytic system after 150 min. In addition, the various undesirable byproducts were depressed when V-TiO_2 photocatalyst was used compared to that in the non-catalytic system.

Key words: V-TiO_2, NH_3 Photodecomposition, Plasma-photocatalytic Hybrid System

INTRODUCTION

Ammonia is a serious pollutant of wastewater that brings about the eutrophication of rivers and lakes [1,2], and its odor has negative effects on humans. With the increasing importance of ammonia removal, various treatments such as biological techniques, adsorption, and thermal incineration have been applied. Recently, the catalytic decomposition of ammonia in wastewater by using metal-TiO_2 photocatalysts has attracted much research attention [3-6]. Most researchers are attempting to transform all ammonia molecules into N_2 via the photocatalytic redox reaction $4\ NH_3+3\ O_2 \rightarrow 2\ N_2+6\ H_2O$. However, it has been reported that when metal-incorporated TiO_2 photocatalysts are used to decompose ammonia, considerable amounts of NO, NO_2, and HNO_3 are formed. Consequently, new photocatalysts are needed to eliminate NO_x compounds, which cause secondary contamination. Previously, we attempted to introduce V-TiO_2 for the photodecomposition of methyl orange, which has a nitrogen component [7]. We discovered that the addition of vanadium to the TiO_2 framework improved the photodecomposition of nitrogen compounds compared to pure TiO_2.

On the other hand, extensive research has also been performed to develop a more effective and low-cost method of VOC decomposition. In recent years, several papers have established that these problems can be overcome by using discharge plasma as the driving light source for photocatalysis [7,8]. Strong plasma is likely to elevate the excited rate of the electrons on the surface of the TiO_2 catalyst, compared with UV irradiation. The emission of UV region energy is similar to that of a UV lamp, with a corresponding range of 3-4 eV [9]. It is believed that photocatalysis is possible using plasma as a light source. Consequently, VOC decomposition can be enhanced. This system, however, continues to encounter some problems. One important issue in using the plasma process for removing VOC involves the treatment of inorganic and organic by-products that are emitted in the process.

The main objective of this study is to enhance the highly concentrated NH_3 (1,000 ppm) decomposition activity in its gas phase by using the dielectric barrier discharge (DBD), plasma-photocatalytic, hybrid system. We produced pure TiO_2 and V (1, 5, and 10 mol-%)-TiO_2 photocatalysts using a common sol-gel method. To confirm the relationship between the physical properties of the photocatalysts and their catalytic decomposition of NH_3, the photocatalyst were analyzed by X-ray diffraction (XRD), UV-visible spectra, thermal gravimetric analysis (TGA), and ammonia temperature-programmed desorption (NH_3-TPD). In addition, the intermediates formed during NH_3 destruction in the plasma-photocatalytic, hybrid system were determined by Fourier transform infrared (FT-IR) spectroscopy, to determine the mechanism of the NH_3 photodecomposition over these photocatalysts.

EXPERIMENTAL

1. Preparation of TiO_2 and V-TiO_2 Photocatalysts

TiO_2 and (1.0, 5.0, 10.0 mol-%)V-TiO_2 photocatalysts were prepared with a conventional sol-gel method to insert vanadium into the TiO_2 framework, as shown in Fig. 1. To prepare the sol mix-

†To whom correspondence should be addressed.
E-mail: mskang@ynu.ac.kr

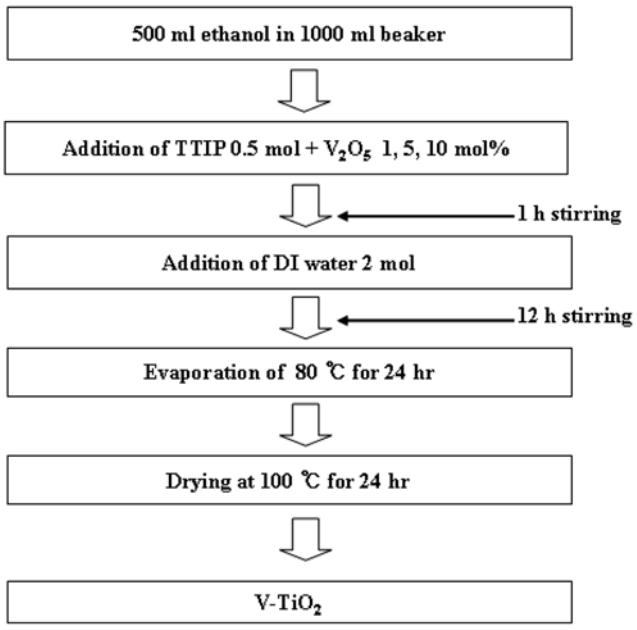

Fig. 1. The preparation of V-TiO_2 photocatalyst using a sol-gel method.

ture, titanium tetraisopropoxide, (TTIP, 99.95%, Junsei Chemical, Tokyo, Japan) and vanadium oxide (99.9%, V_2O_5, Junsei Chemical, Japan) were used as the titanium and vanadium precursors, respectively, and ethanol (99.9%, Wako Pure Chemical, Osaka, Japan) was used as the solvent. To 500 ml of ethanol were added 0.5 mol TTIP and 1.0, 5.0, or 10.0 mol% V_2O_5, after which 2.0 mol distilled water was added to cause hydrolysis. Finally, the solution was adjusted to pH=3.0. The final solution was evaporated at 80 ℃ for 24 h. The resulting yellowish precipitate was dried at 100 ℃ for 24 h, and finally heated at 500 ℃ for 3 h for crystallization of the anatase structure.

2. Characterizations of TiO_2 and V-TiO_2 Photocatalysts

The synthesized TiO_2 and V-TiO_2 powders were subjected to XRD (model PW 1830; Philips, Amsterdam, The Netherlands) analysis with nickel-filtered, Cu$K\alpha$ radiation (30 kV, 30 mA) at 2θ angles from 5 to 70°. The scan speed was 10° min^{-1} and the time constant was 1 s. The sizes and shapes of the TiO_2 and V-TiO_2 particles were observed by using scanning electron microscopy (SEM, model JEOL-JSM35CF; Tokyo, Japan) with the power set to 15 kV. UV-visible spectra of the TiO_2 and V-TiO_2 powders were obtained with a Shimadzu MPS-2000 spectrometer (Kyoto, Japan) with a reflectance sphere over the spectral range from 200 to 800 nm.

The Brunauer, Emmett, and Teller (BET) surface area and pore size distribution (PSD) of the TiO_2 and V-TiO_2 powders were measured by nitrogen gas adsorption with a continuous flow method using a chromatograph equipped with a thermal conductivity detector (TCD) at liquid-nitrogen temperature. A mixture of nitrogen and helium was used as the carrier gas with a MicroMetrics Gemini 2375 (Londonderry, NH, USA). The sample was treated at 350 ℃ for 3 h before nitrogen adsorption.

NH_3-TPD measurements of TiO_2 and V-TiO_2 were carried out on a conventional TPD system equipped with a TCD cell. The catalysts were exposed to He gas at 350 ℃ for 2 h in order to remove water and impurities on the surface. After pretreatment, the samples were exposed to ammonia at room temperature for 2 h, and then heated at 10 ℃/min to 500 ℃. The amount of desorbed gas was continuously monitored with a TCD cell.

3. Analysis of Ammonia Decomposition over TiO_2 and V-TiO_2 in a Plasma-photocatalytic Hybrid System

The decomposition of NH_3 was performed with a flow reactor (Fig. 2) composed of an emitting stainless steel rod held at the center of the reactor, a thin wrapping wire sheet, and small beads. The reactor was made of quartz glass cylinders of diameter 25 mm and length 240 mm. A high-voltage AC current was supplied with an amplifier (KSA-15/05CA) and a function generator (EZ digital, FG-7002C). The waveforms of the pulse voltage and current were meas-

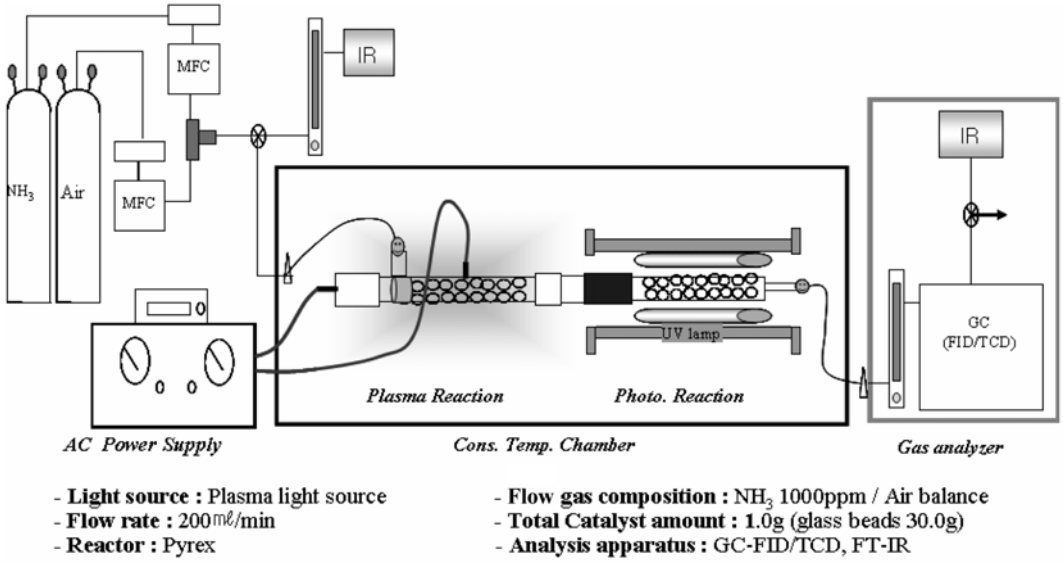

Fig. 2. Schematic diagram of the experimental apparatus of the dielectric barrier discharge, plasma-photocatalytic, hybrid system for the decomposition of NH_3.

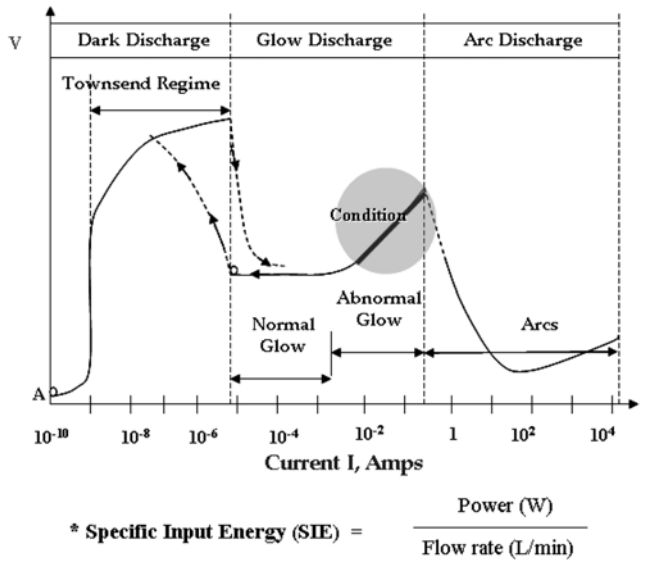

Fig. 3. Condition of the dielectric barrier plasma generation for the decomposition of NH_3.

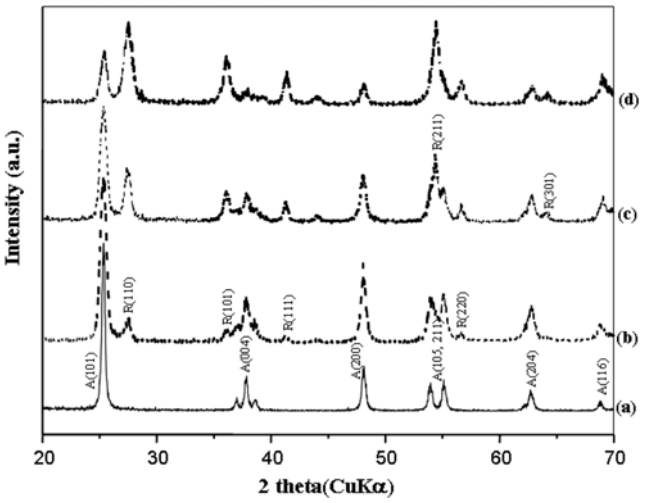

Fig. 4. XRD patterns of V-TiO_2 (V/Ti=1, 5, 10 mol-%) photocatalysts. (a) TiO_2, (b) 1 mol-% V-TiO_2, (c) 5 mol-% V-TiO_2, and (d) 10 mol-% V-TiO_2.

ured with a digital oscilloscope with a voltage divider and current probe. The input power was measured by using a digital power meter located at the wall plug of the transformer. This input value measured the discharge power and energy loss in the power source. The radiation power generated was measured by regulating the current and pulse voltage. The V-Q method was used to determine the discharge power in the plasma reactors. The charge Q was determined by measuring the voltage across the capacitor of 1 μF, which was connected sequentially to the ground line of the plasma reactors [10]. The energy was transferred from the power source to the plasma reactor at a rate of 20-30%. The intensity of the pulse voltage was measured at 7.0 kV, while the frequency of the currents was determined at 600 Hz. The discharge power was calculated by multiplying the area of the V-Q parallelogram by the frequency. The specific input energy (SIE), which is shown in Fig. 3, was calculated based on the following equation:

$$\text{Specific input energy (J/L)} = \frac{\text{Discharge power (W)}}{\text{Gas flow rate (L/min)}}. \quad (1)$$

The SIE value was adjusted by changing either the applied voltage or the frequency [11].

A quartz cylinder photo-reactor, 36 cm in length and 1.0 cm in diameter, was used and UV lamps (model BBL, 365 nm, 24(6×4)W/m^2, 20 cm length×1.5 cm diameter, Shinan Co., Korea) were used for the photoreaction. The amount of coated catalyst on the glass beads was set at 0.5 g (total 30.0 g). NH_3 concentration was set at 1,000 ppm. In a continuous system, air was used as the carrier gas at a flow rate of 150 mL/min.

The ammonia concentrations before and after photodecomposition were analyzed by gas chromatography (GC17A; Shimadzu, Kyoto, Japan) with flame-ionization/thermal-conductivity detectors (FID/TCD) (HP-1 capillary column). The percentage removed was calculated from the disappearance of the pollutant during the decomposition process. All experiments were performed at room temperature and atmospheric pressure. FT-IR spectrometry (FTIR-8400; Shimadzu) and GC/MS were used to quantify the products after ammonia decomposition at a reaction time of 60 min.

RESULTS AND DISCUSSION

1. Characteristics of the TiO_2 and V-TiO_2 Photocatalysts

Fig. 4 shows the XRD patterns of the TiO_2 and V-TiO_2 photocatalysts. Photocatalytic TiO_2 samples with anatase and rutile structures were used to decompose volatile organic compounds (VOCs). Most samples belonged to the mixture of anatase and rutile structures, except pure TiO_2 with only anatase structure. However, the ratios of the peak intensities of A(anatase)/R(rutile) were distinguishable and they decreased with increasing vanadium component. In particular, the peaks were also broadened with increasing vanadium component. Generally, the crystallites are reduced in size as the peaks are broadened. The peaks assigned to V_2O_5 were not seen in all samples of the V-TiO_2s, indicating that the vanadium ions were well inserted into the TiO_2 framework for vanadium concentrations of up to 10.0 mol-%.

SEM photographs of TiO_2 and V-TiO_2 photocatalysts are shown in Fig. 5. The images unfortunately are not clear because of the low resolution of the instrumental equipment. However, all the catalysts were confirmed to be relatively uniform and spherical. The pure TiO_2 particles were the smallest, and the particle size increased with increasing vanadium addition. This result is contrary to the XRD result presented in Fig. 4 and was attributed to the presence of particles between the anatase and rutile structures.

Table 1 summarizes the physical properties of the TiO_2 and V-TiO_2 photocatalysts. First, the true atomic percentages of vanadium/titanium, which were determined by using the inductively coupled plasma (ICP), were 1.01, 5.97, and 8.98 in V 1.0, 5.0, and 10.0 mol-% added TiO_2, respectively. The bulk pores generated between each particle ranged from 101 to 52 nm with pore volumes ranging from 0.03 to 0.07 cm^2/g. Despite these bulk pores, the surface areas were very small and they decreased with increasing vanadium content.

Fig. 6 shows the UV-visible spectra of the TiO_2 and V-TiO_2 pho-

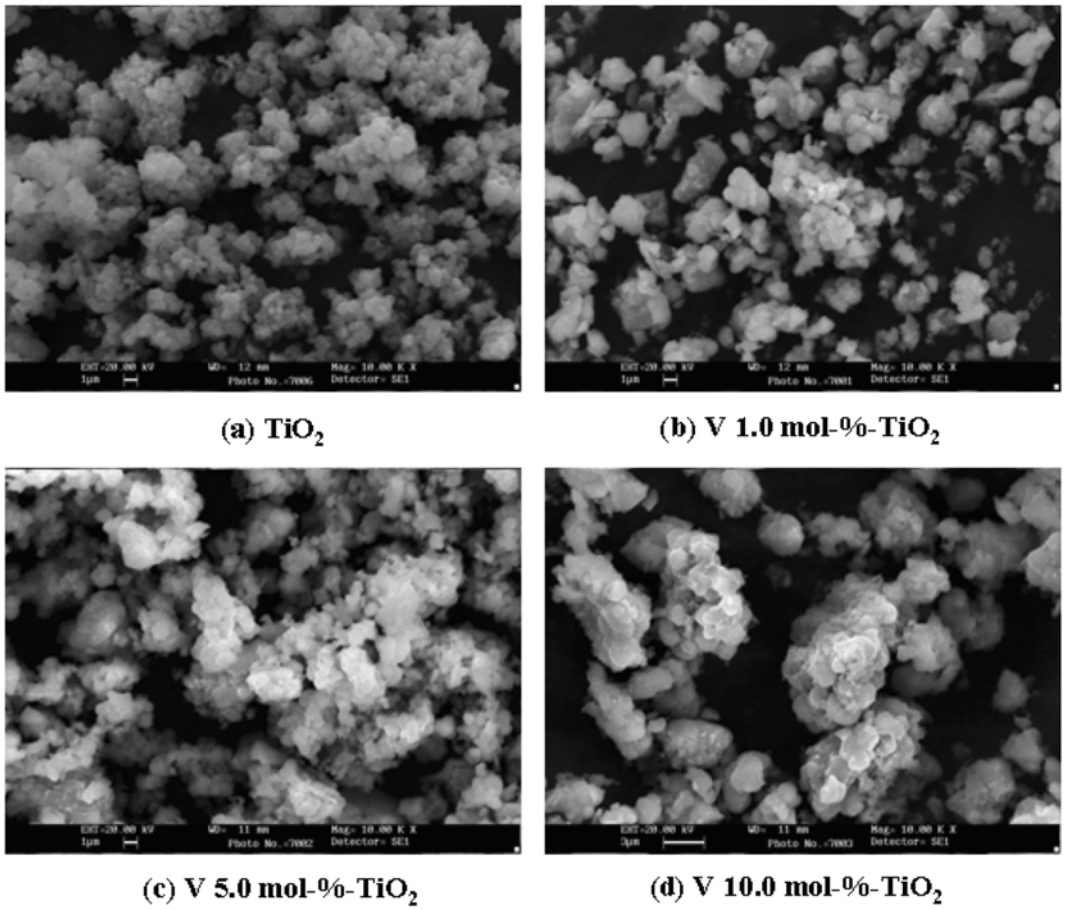

Fig. 5. SEM images of V-TiO_2 photocatalysts (V/Ti=1, 5, 10 mol-%).

Table 1. Physical properties of the prepared V-TiO_2 photocatalysts

Catalyst	Compositions in powder	Surface area	Pore volumee	Peak pore size
	V/Ti	(m^2/g)	(cm^3/g)	(nm)
TiO_2	-	48.20	0.07	52.1
V 1.0 mol-%-TiO_2	1.01	11.88	0.03	101.4
V 5.0 mol-%-TiO_2	5.97	27.41	0.04	72.5
V 10.0 mol-%-TiO_2	8.98	28.18	0.05	64.6
Experimental method	ICP	BET	N_2 adsorption	N_2 adsorption

tocatalyst particles. The absorption of Ti^{4+} tetrahedral symmetry normally appears at around 350 nm. In the figure, the absorption band is around 360 nm in pure TiO_2. Moreover, the absorption bands are shifted to a higher wavelength in V-TiO_2 compared to that in pure TiO_2. In addition, the shift was more significant in V 10.0 mol-%-TiO_2. Generally, the band gaps in a semiconductor material are closely related to the wave range absorbed; the band gap is shortened at higher absorption wavelengths. Therefore, we postulate that vanadium addition lowered the band gap energy and, consequently, the photo-catalysts could be activated at a weak energy, such as that of visible light.

To confirm the effect of the addition of vanadium to the TiO_2 framework, the NH_3-TPD test was performed. Fig. 7 shows the resulting profiles. General, these profiles have two parts: one that appears at temperatures of 100 to 150 °C, which is related to physical adsorption, and another that appears at temperatures of 300 to 400 °C. It is well known that the low and high temperature peaks correspond to the weak and strong acid sites, respectively. With increasing vanadium component, the bands were shifted to the high temperature in this study. In addition, the NH_3 adsorption was the highest in 5.0 mol-% V-TiO_2, indicating that vanadium generated new acid sites on the TiO_2 framework, which increased the acid strength with increasing vanadium concentration.

2. Decompositions of Ammonia over TiO_2 and V-TiO_2 Catalysts

Fig. 8a shows the catalytic performance for ammonia (1,000 ppm) removal without photocatalyst in a plasma-only system with applied plasma voltage. Without catalyst, the ammonia removal increased

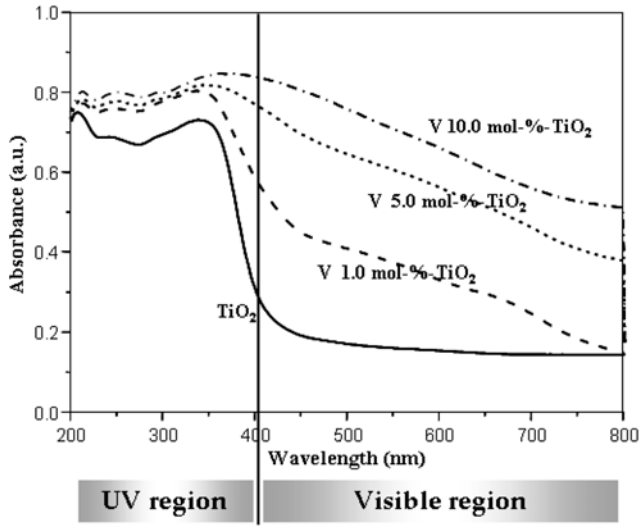

Fig. 6. UV-visible spectra patterns of V-TiO_2 (V/Ti=1, 5, 10 mol-%) photocatalysts.

with increasing applied voltage. The ammonia level remained at 400 ppm at 5 and 7 kV after 400 min, while more than 90% of the introduced ammonia was removed at 10 kV after 400 min. FT–IR analyses were used to determine the products of ammonia photodecomposition after 1 h, as shown in Fig. 8a, and the result is displayed in Fig. 8b. Intermediates such as NO_2, $-NH_2^+$, -NH, and NO are seen in this figure. With applied plasma voltage, oxidized intermediates appeared and the directly formed NO was increased at 10 kV compared to at the lower plasma voltage.

Fig. 9 shows the activity of NH_3 decomposition in a photocatalytic-only system (a) and plasma-photocatalytic, hybrid system (b) at an applied voltage of 10 kV. First, in (a), the rate of NH_3 removal was slower than that in the plasma system for all catalysts. Over pure TiO_2, NH_3 was reduced to about 65% after 170 min. However, the decomposition rate was faster and the removed amount was greater in V-TiO_2. The NH_3 removal rate reached 95% after 170 min when 10.0 mol-% V-TiO_2 was used. On the other hand, the removal rate was remarkably enhanced in the plasma-photocatalytic, hybrid system (b). Despite the absence of any catalyst, an

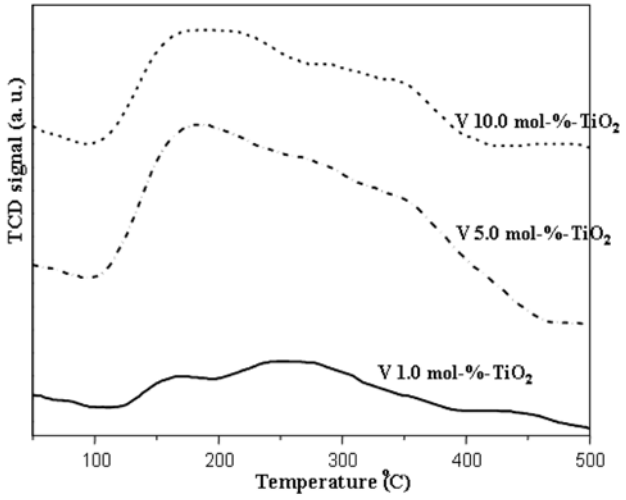

Catalysts	NH_3 desorption amount (Area/g)
V 1 mol-%-TiO_2	1.27×10^5
V 5 mol-%-TiO_2	4.18×10^5
V 10.0 mol-%-TiO_2	2.46×10^5

Fig. 7. NH_3-TPD spectra of V-TiO_2 photocatalysts (V/Ti=1, 5, 10 mol-%).

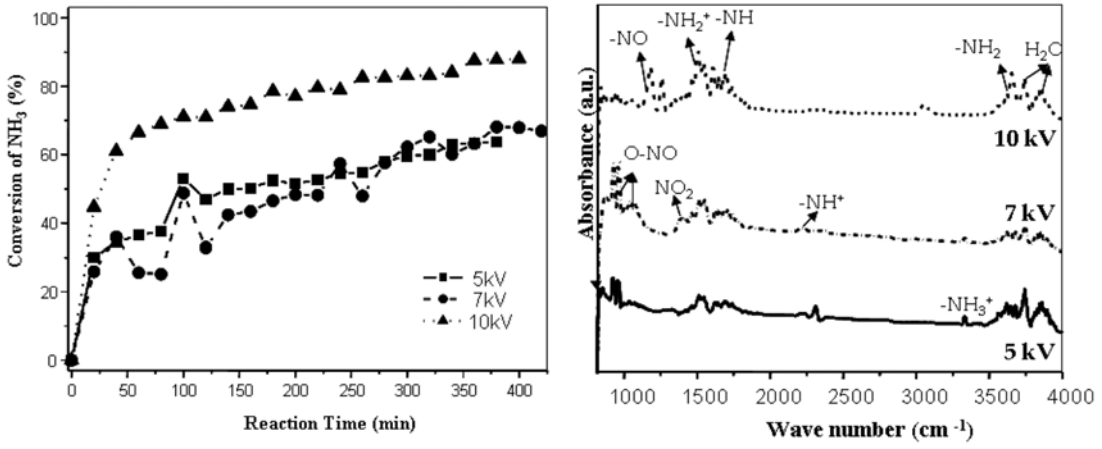

(a) Catalytic performance on NH_3 decomposition **(b) FT-IR spectra during NH_3 removal on basis of (a)**

Fig. 8. Optimal applied voltage for NH_3 decomposition in the plasma system and comparison of FT-IR spectra under NH_3 decomposition at various applied voltages.

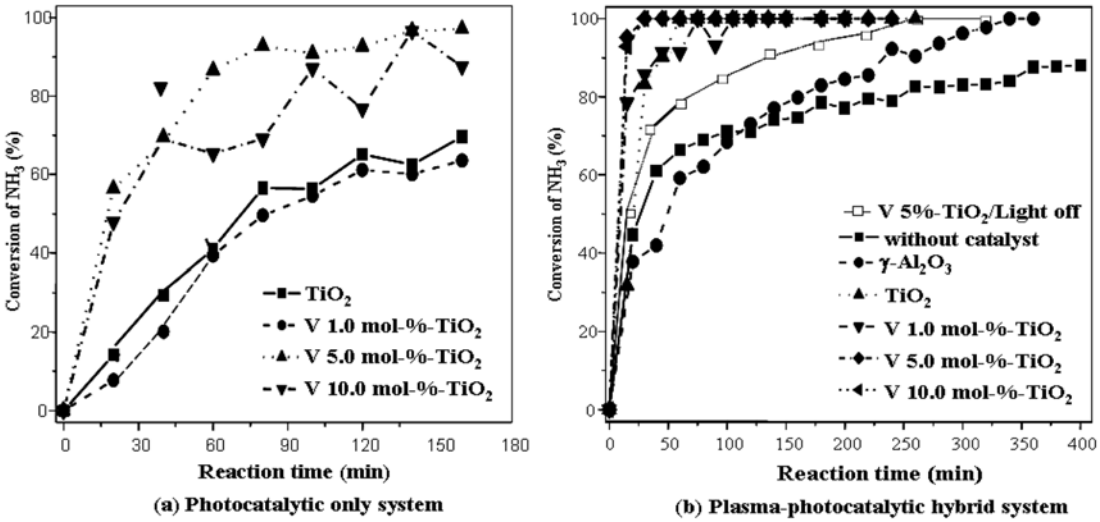

Fig. 9. Comparison of NH_3 decomposition in the photocatalytic and plasma-photocatalytic, hybrid system at applied voltage of 10 kV.

Path I (general photo-oxidation)		
Initiation Steps	**Propagation Steps**	**Termination Steps**
$O_2 \rightarrow 2O\bullet$ ⇝ $+ H_2O \rightarrow 2\,OH\bullet$ ⇝ $2O\bullet$	3) $\bullet NH_2 + \bullet O \rightarrow NH_2O$	
	4) $\bullet NH + \bullet O \rightarrow NHO$	
	5) $\bullet NH_2 + \bullet OH \rightarrow NH_3O + \bullet O \rightarrow NHO + H_2O$	7) $NH_2O + NH_2O \rightarrow N_2 + 2H_2O$
1) $NH_3 + \bullet OH \rightarrow NH_4O\bullet \rightarrow \bullet NH_2 + H_2O$	6) $\bullet NH + \bullet OH \rightarrow NH_2O + \bullet O \rightarrow \bullet NO + H_2O$	8) $NHO + NHO \rightarrow N_2O + H_2O$
		9) $\bullet NO + \bullet NO \rightarrow N_2 + O_2$
2) $NH_3 + \bullet O \rightarrow NH_3O\bullet \rightarrow \bullet NH + H_2O$		10) $\bullet NO + \bullet O \rightarrow NO_2$
Path II (directly decomposition by strong plasma radiation)		
$O_2 \rightarrow 2O\bullet$		
$NH_3 \rightarrow \bullet N + H_2 + \bullet H$		
$\bullet H + \bullet OH \rightarrow H_2O$		
$\bullet NH_2 + \bullet OH \rightarrow NH + H_2O \rightarrow NH + O \rightarrow NHO$		
$\bullet NH_2 + \bullet O \rightarrow NH_2O$		
$NHO + NHO \rightarrow N_2O + H_2O$		
$NH_2O + NH_2O \rightarrow N_2 + 2H_2O$		
$\bullet N + O\bullet = NO$		

Scheme 1. The expected NH_3 decomposition mechanism in the plasma system.

NH_3 decomposition of 80% was achieved after 400 min. In addition, the removal reached 100% for all the vanadium-loaded photocatalysts after 120 min.

CONCLUSIONS

Based on GC, FT-IR, and GC/MS results, we have suggested a mechanism for NH_3 plasma-decomposition, as shown in Scheme 1. Two oxygen and one hydroxyl radicals generated by plasma-radiation attack the NH_3 molecules, which leads to the formation of NH_2 and NH radicals (steps 1 and 2). These NH and NH_2 radicals are transformed into NHO and NH_2O molecules, and NO radical, as intermediates, via the respective attack of oxygen and hydroxyl radicals (steps 3-6). Finally, N_2 N_2O, NO, and NO_2 are produced by the reaction between two NH_2O, NHO, NO molecules (steps 7-9), and NO and O radicals (step 10), respectively. In addition, the NH_3 molecules are directly cleaved by strong plasma radiation, as shown in Path II. From this result, it was consequently realized that unlike the photocatalytic reaction, the plasma condition generated undesirable molecules, such as NO_x, as secondary products. This is a serious problem in the proposed method for photocatalytic ammonia removal using the DBD, plasma-photocatalytic, hybrid system, which will require solution before the system can be practically applied.

ACKNOWLEDGMENT

This work was supported by the Korea Research Foundation (KRF-2003-D00015), for which the authors are very grateful.

REFERENCES

1. P. I. Riggan, R. N. Lockwood and E. N. Lopez, *Environ. Sci. Technol.*, **19**, 971 (1985).
2. Y.-H. Son, M.-K. Jeon, J.-Y. Ban, M. Kang and S.-J. Choung, *J. Ind. Eng. Chem.*, **11**, 938 (2005).
3. M. Kang, *Appl. Catal. B: Environ.*, **37**, 187 (2002).
4. J. H. Lee, W. S. Nam, M. Kang, G. Y. Han, M.-S. Kim, K. Ogino, S. Miyata and S.-J. Choung, *Appl. Catal. A: General*, **244**, 49 (2003).
5. S.-H. Park, S.-C. Lee, M. Kang and S.-J. Choung, *J. Ind. Eng. Chem*., **10**, 972 (2004).
6. M.-K. Yeo and M. Kang, *Water Research*, **40**, 1906 (2006).
7. Y. S. Mok, H. C. Kang, M. H. Cho and I. S. Nam, *Korean J. Chem. Eng.*, **20**, 239 (2003).
8. S. G. Jeon, K. H. Kim, D. H. Shin, N. S. Nho and K. H. Lee, *Korean J. Chem. Eng.*, **24**, 522 (2007).
9. J.-Y. Ban, S.-J. Choung and M. Kang, *Appl. Surf. Sci.*, **253**, 535 (2006).
10. N.-L. Wu, M.-S. Lee, Z.-J. Pon and J.-Z. Hsu, *J. Photochem. Photobiol. A: Chem.*, **163**, 277 (2004).
11. Q. Liu, X. Wu, B. Wang and Q. Liu, *Mater. Res. Bull.*, **37**, 2255 (2002).